Metasomatic wolfeite and associated phosphates from the Otov I granitic pegmatite, western Bohemia

Metasomatický wolfeit a sdružené fosfáty z granitického pegmatitu Otov I v západních Čechách

(12 text-figs, 9 tabs)

MORGAN MASAU[1] – JOSEF STANĚK[2] – PETR ČERNÝ[1] – RON CHAPMAN[1]

[1] *Department of Geological Sciences, University of Manitoba, Winnipeg, MB, Canada R3T 2N2*
[2] *Department of Mineralogy, Petrology and Geochemistry, Masaryk University, Kotlářská 2, 611 37 Brno, Czech Republic*

The pegmatite Otov I, outcropping on Větrný vrch at the village of Otov, western Bohemia, belongs to the beryl-columbite-phosphate subtype of rare-element granitic pegmatites with rare spodumene. To date, twenty species of phosphates were identified in this pegmatite, and twelve others were recognized during the present study. Wolfeite is established here as a significant metasomatic mineral with average Mn/(Mn+Fe)(at.) of 0.46, F content largely below the detection limit of electron microprobe, α 1.741, β 1.743, γ 1.746, $\gamma - \alpha$ 0.005, (+)2V medium (calc. 37°), *a* 12.327(3), *b* 13.225(3), *c* 9.845(2) Å, β 108°23', *V* 1522.95(47) Å^3. The primary precursor of wolfeite was (I) arrojadite-dickinsonite studded with sporadic grains of zircon (with inclusions of uraninite) and sphalerite (with droplets of chalcopyrite). Arrojadite-dickinsonite was first veined by (II) a very fine-grained assemblage of muscovite, (Fe, Mn, Al, Ca, Mg, Li)-bearing phosphates (lazulite-scorzalite, eosphorite, samuelsonite?, triphylite, montebrasite) and minor calcite. Subsequent replacement of most of the arrojadite-dickinsonite generated (III) fine-grained wolfeite with interstitial F-bearing hydroxylapatite. Partial replacement of triphylite by alluaudite, hagendorfite and UK-D was coeval with, and spatially preceded, wolfeite metasomatism. Late low-temperature (IV) replacements and veinings permeating the preceding assemblages include ludlamite, goyazite, hydroxylchlorapatite, fairfieldite? and chlorite?. The whole phosphate assemblage is remarkably poor in F, but enriched in Cl in late stages, and it is generally strongly reduced. Substantial contents of Ca, Mg, Sr and Cl, in the virtual absence of Ba, indicate contamination by components of the gabbroic wallrock at both magmatic and late hydrothermal stages.

Key words: wolfeite, arrojadite, dickinsonite, lazulite, samuelsonite, triphylite, apatite, alluaudite, goyazite, granitic pegmatite, Bohemia, Czech Republic

Introduction

The Otov I pegmatite has been known since some 50 years ago (Weber 1948) for its diversified assemblage of primary, secondary and supergene phosphate minerals, some of which were more or less thoroughly described in the literature. Novotný et al. (1951) described triphylite, and Novotný (1956) reviewed this mineral and its alteration products sicklerite and heterosite. Staněk (1960) examined montebrasite, augelite and lazulite, whereas Čech et al. (1961) focused their attention at lipscombite. Čech (1981) summarized the phosphate assemblage and associated minerals.

However, one of the prominently missing links in phase descriptions and paragenetic relations is wolfeite and associated phosphates. In the present paper, wolfeite and its phosphate entourage are characterized individually and in their paragenetic relationships; the Otov I wolfeite is documented as a metasomatic mineral, which is not necessarily the case at other localities.

The parent pegmatite

The Otov I pegmatite belongs to the Poběžovice – Domažlice pegmatite population hosted by mica schists and plagioclase paragneisses of the Domažlice crystalline complex, penetrated locally by gabbroic to granitoid intrusions (Vejnar 1965; West-Bohemian pegmatite field of Novák et al. 1992). Otov I is classified as the beryl-columbite-phosphate subtype of rare-element granitic pegmatites, verging on the spodumene subtype of complex pegmatite type (Novák et al. 1992).

The pegmatite body was examined in detail by Vejnar (1965). This author characterizes Otov I as an irregular, E–W striking and north-dipping dike, about 300 m long, 5 to 30 thick, and disclosed by mining and drilling to a depth of ~50 m. Numerous offshoots of the dike penetrate the wallrocks. Contacts of the dike with enclosing lithologies are usually sharp, locally extensively mylonitized; the wall rock is in these cases strongly affected by hydrothermal alteration.

The pegmatite is distinctly zoned but in an extremely irregular manner (Vejnar 1965). The border zone is poorly developed, largely just a few cm wide; it consists of medium- to coarse-grained aggregates of feldspars and quartz (Plg + Kf + Qtz). Outer intermediate zone, variable from 2 to 10 m in thickness, comprises a very coarse-grained quartzofeldspathic assemblage with biotite and abundant muscovite, accumulated particularly in the hanging-wall parts of the dike (Plg + Kf + Qtz + Bi + Mu). This zone grades inwards into the inner intermediate zone, 3 to 5 m thick, by gradual disappearance of micas and coarsening of the K-feldspar (Kf + Qtz + Plg). Very coarse to blocky K-feldspar is the dominant component here, locally intergrown with graphic quartz. Accumulations of coarse tabular muscovite are found close to the quartz core. The pods of quartz core attain 1 to 5 m, rarely somewhat larger dimensions; they con-

tain sparse crystals of K-feldspar several metres in size. The contacts of the inner intermediate unit with the quartz core are decorated by crystals of beryl, pods of Fe-Mn-Ca-Li phosphates and other accessory minerals.

Examination of the pegmatite by the second author (in the nineteen fifties and sixties) shows that microcline-perthite, albite and quartz are the most common rock-forming minerals; muscovite is much less abundant (although present in several generations), and biotite even less widespread. All of the other minerals occur only locally, including the slightly more abundant beryl, Fe-Mn-Ca-Li phosphate pods and garnet (almandine to spessartine). Spodumene forms crystals up to 70 cm in size but was only found in a single spot. Granular cassiterite rarely forms dm-size intimate intergrowths with yellow sphalerite. Tabular crystals of ferrocolumbite, up to 7 cm long, are very rare, as is zircon, gahnite and possible monazite.

The phosphate minerals form pods and vein-like aggregations up to 0.5 m across. According to Staněk (1960) and Čech (1981), greyish-green triphylite and pale-brown intergrowths of graftonite and sarcopside are the dominant phases, along with wolfeite, apatite and montebrasite. Hydrothermal alteration yielded numerous metasomatic and secondary phases: ferrisicklerite, heterosite, apatite, vivianite, lipscombite, griphite, fairfieldite, lazulite, and rockbridgeite. Augelite was identified in montebrasite. Sulphides were commonly associated with both primary and secondary phosphates: pyrite, pyrrhotite and chalcopyrite. Supergene weathering generated probable strengite, dufrenite and cacoxenite at the expense of preexisting phosphates. Chalcopyrite locally decomposed into malachite and torbernite, and associated autunite is very rare.

The present study expands the phosphate mineralogy of Otov I by nine species and three unknown phases, all closely associated with wolfeite.

Experimental

Electron-microprobe analyses were performed on the Cameca SX-5 instrument at the Department of Geological Sciences, University of Manitoba, using a 10 μm beam, operating voltage of 15 kV and sample current of 20 nA. Standards used were maricite (Na$K\alpha$, Fe$K\alpha$), olivine (Mg$K\alpha$), brazilianite (Al$K\alpha$), diopside (Si$K\alpha$), Wilberforce apatite (Ca$K\alpha$, F$K\alpha$, P$K\alpha$), tugtupite (Cl$K\alpha$), orthoclase (K$K\alpha$), spessartine (Mn$K\alpha$), gahnite (Zn$K\alpha$), $SrTiO_3$ (Sr$L\alpha$), and barite (Ba$L\alpha$). In most cases, counting time was 20 s for Na, Si, P, Fe and Mn, 40 s for K, Mg, Al, Ca, Zn, Sr, Cl and F, and 10 s for background. Some variations in counting times, however, were introduced for specific mineral compositions. Analytical data were reduced and corrected by aid of the program of Pouchou – Pichoir (1984, 1985). Chemical compositions expressed in the standard wt. % oxides were normalized to atoms per formula unit (*apfu*) or unit-cell contents (*apuc*) in different ways, as deemed suitable for individual species (see Table 1 to 9 below).

Unit-cell dimensions were refined from diffractograms, recorded for Cu$K\alpha_1$ radiation (λ 1.5406 Å) on a Siemens D 5000 diffractometer, using the Appleman – Evans (1973) least-squares program. Internal standards were selected to minimize diffraction overlaps (NBS-silicon-calibrated BaF_2). Single-crystal studies were performed by M. A. Cooper on a Nicolet *P*4 automated 4-circle diffractometer with a CCD detector.

Optical properties were examined in transmitted-light polarizing microscope in thin sections and immersion liquids. Refractive indices were determined for Na-light (λ 589 nm).

Because of the very fine-grained nature of most of the phosphates, electron microprobe and optical checks were commonly the only techniques applicable to their study; X-ray diffraction could be performed only exceptionally. Consequently, the mineral identification depended heavily on the chemical composition, the study of which was hampered by lack of direct data on Li, OH and H_2O. Most phosphates were unambiguously identified, two are probable (their names are accompanied by question marks), and three could not be correlated with any known species (quoted as UK-D, -G, -H). Specific information on the individual cases is given in the descriptive section below.

The phosphate assemblage

To simplify the understanding of the complex relationships among wolfeite and associated phases, we present here a condensed review of the paragenetic sequence of the whole assemblage, followed below by detailed characterization of individual species. This descriptive section will also provide documentation of textural features used to unravel the paragenetic sequence.

The following stages of mineral formation can be distinguished in the available hand specimens of wolfeite:

(I) Primary phases: arrojadite-dickinsonite, zircon (with inclusions of uraninite), sphalerite (with droplets of chalcopyrite), not visible in Fig. 1.

(II) Veining by muscovite (± very minor calcite) and very fine-grained aggregates of lazulite-scorzalite, eosphorite, samuelsonite?, montebrasite (mottled greenish and blue veins in Fig. 1), rimmed by triphylite (dark brown in Fig. 1).

(III) Replacement of most of the arrojadite-dickinsonite by wolfeite (pale-brown with darker brown patches, dominant in Fig. 1) and hydroxylapatite, possibly coeval with alluaudite, hagendorfite and UK-D formed at the expense of triphylite (invisible in Fig. 1).

(IV) Minor microscopic veining and replacement of all preceding phosphates by ludlamite, goyazite, hydroxylchlorapatite, fairfieldite? and chlorite?.

Fig. 1. Wolfeite (dominant, pale to dark brown) with veins of muscovite, lazulite-scorzalite and other phosphates (greenish with blue patches), rimmed by altered triphylite (dark brown borders); note the dirty yellowish and black layers at, and parallel with, the vertical left-hand edge of the sample; very close to actual size.

Descriptive mineralogy

The primary phases (I)

Minerals of the *arrojadite-dickinsonite* series, $KNa_4CaMn^{2+}_4(Fe,Mn)^{2+}_{10}Al(PO_4)_{12}(OH,F)_2$, form corroded to rounded and embayed relics in the muscovite + phosphate veins and in the masses of wolfeite (Figs 2, 3). Three of the six compositions analyzed correspond to the Fe-dominant arrojadite, the other three to the Mn-dominant dickinsonite, but all six are close to the midpoint of the series. The chemical compositions normalized to 12 P + 50 anions closely match the ideal formula of this series, with slight excess of (OH, F, Cl) over 2 *apfu* (Table 1). This surplus can be avoided by conversion of adequate proportion of Fe^{2+} to Fe^{3+}, but the resulting percentage of Fe_2O_3 is very high and so far unknown in this mineral group (Table 1). However, most analyzed samples of arrojadite-dickinsonite contain Li in distorted tetrahedral coordination (Moore et al. 1981), and complementing the total of (Mg, Fe, Mn, Zn) to 14.000 by Li substantially (but not completely) alleviates the problem of excessive (OH, F, Cl). This last normalization quoted in Table 1 is probably the best approximation to the real composition of the Otov I arrojadite-dickinsonite samples. Single-crystal X-ray diffraction gave unit-cell dimensions a 24.829(1), b 10.0580(8), c 16.629(1) Å, β 105.673(3)°, V 3998.4(7) Å^3. These values are intermediate between those quoted for distinctly Fe-dominant arrojadite and explicitly Mn-rich dickinsonite in the literature (Moore et al. 1981).

Fig. 2. Relictic arrojadite-dickinsonite (near-black, center) surrounded and penetrated by wolfeite (grey); white specks are sphalerite. Scale bar is 500 μm long.

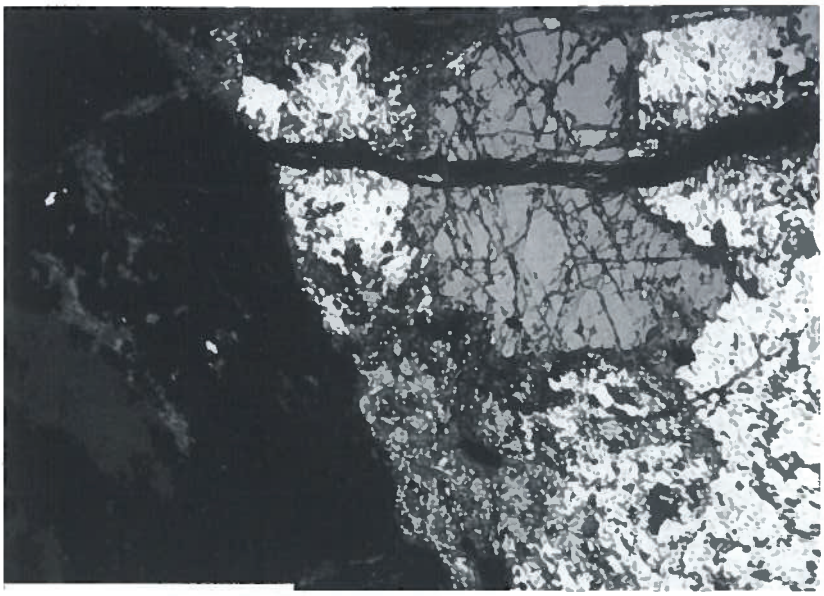

Fig. 3. Arrojadite-dickinsonite (grey, right of center) replaced by wolfeite (white), both crosscut by ludlamite (black vein). Ludlamite also composes a part of the black area on the left side, which consists primarily of triphylite, with indistinguishable goyazite and dark-grey chlorite?; mottled grey patches belong to altered hagendorfite. Scale bar is 500 μm long.

Table 1. Chemical composition of arrojadite (21) and dickinsonite (57), normalized in three different modes:
* to 12P + 50 anions + 2(OH,F,Cl) compensated by calculated Fe^{3+}, and ** to 12P + 50 anions + Σ (Mn, Fe, Mg, Zn, Li) = 14 to minimize the excess of (OH, F, Cl); † = calculated

	21	57	21*	57*	21**	57**
P_2O_5	40.70	40.17	40.70	40.17	40.70	40.17
SiO_2	0.03	0.00	0.03	0.00	0.03	0.00
Al_2O_3	2.33	2.42	2.33	2.42	2.33	2.42
Fe_2O_3†	–	–	3.36	6.23	–	–
MgO	2.79	1.41	2.79	1.41	2.79	1.41
CaO	2.27	2.37	2.27	2.37	2.27	2.37
MnO	19.22	21.44	19.22	21.44	19.22	21.44
FeO	23.52	20.82	20.49	15.21	23.52	20.82
ZnO	0.05	0.04	0.05	0.04	0.05	0.04
SrO	0.00	0.26	0.00	0.26	0.00	0.26
Li_2O†	–	–	–	–	0.01	0.49
Na_2O	5.47	5.65	5.47	5.65	5.47	5.65
K_2O	1.93	2.12	1.93	2.12	1.93	2.12
F	0.45	0.00	0.45	0.00	0.45	0.00
Cl	0.02	0.02	0.02	0.02	0.02	0.02
H_2O†	0.98	1.54	0.64	0.84	0.98	1.54
O=F	-0.19	0.00	-0.19	0.00	-0.19	0.00
O=Cl	0.00	0.00	0.00	0.00	0.00	0.00
Total	99.38	99.10	99.57	98.18	99.39	99.59
atoms per formula unit						
P	12.000	12.000	12.000	12.000	12.000	12.000
Si	0.010	0.000	0.010	0.000	0.010	0.000
Σ	12.010	12.000	12.010	12.000	12.010	12.000
Al	0.956	1.006	0.956	1.006	0.956	1.006
K	0.858	0.954	0.858	0.954	0.858	0.954
Na	3.694	3.865	3.694	3.865	3.694	3.865
Ca	0.847	0.896	0.847	0.896	0.847	0.896
Sr	0.000	0.053	0.000	0.053	0.000	0.053
Σ	0.847	0.949	0.847	0.949	0.847	0.949
Mg	1.449	0.742	1.449	0.742	1.449	0.742
Fe^{2+}	6.850	6.144	5.969	4.489	6.850	6.144
Fe^{3+}	–	–	0.881	1.655	–	–
Mn	5.670	6.408	5.670	6.408	5.670	6.408
Zn	0.013	0.010	0.013	0.010	0.013	0.010
Li	–	–	–	–	0.018	0.696
Σ	13.982	13.304	13.982	13.304	14.000	14.000
F	0.496	0.000	0.496	0.000	0.496	0.000
Cl	0.012	0.012	0.012	0.012	0.012	0.012
OH	2.295	3.642	1.493	1.988	2.277	2.946
O	47.198	46.346	49.493	49.988	47.216	47.042
Σ	50.001	50.000	51.494	51.988	50.001	50.000

Zircon composes subhedral, somewhat rounded grains enclosed in wolfeite. The grains are homogeneous, but they contain numerous tiny inclusions of *uraninite*. Zircon is fresh, apparently non-metamict, yielding near-perfect wt. % totals and stoichiometry when normalized to 4 oxygen atoms (Table 2). This seems to be remarkable in view of the appreciable content of the actinide elements in zircon, and of the copious abundance of uraninite inclusions. The Hf and P contents of zircon are low, and Y plus REE's are at or below detection limits. The values of the Zr/Hf (wt.) ratio average at 10.9. Uraninite also gives a good empirical formula, despite its rather high Pb content (Table 2); the somewhat high total of cations per 4 oxygen atoms suggests that some U may be present in an oxidation state higher than 4+. However, data on uraninite are scarce as most of its grains cannot be analyzed because of their minute dimensions and a virtual certainty of beam overlap into the enclosing zircon.

Sphalerite forms irregular grains up to 1 mm in size, enclosed in wolfeite, and minute grains 5 to 20 μm in size dispersed in wolfeite and in the muscovite + phosphate veins. The composition of sphalerite shows a steady but low content of Fe, minor Mn and modest Cd in the large grains (average Zn/Cd 129), whereas the dispersed minute granules have higher Fe and particularly Mn, and somewhat lower Cd (average Zn/Cd 178; Table 3).

Droplets of *chalcopyrite* evenly dispersed in the large grains of sphalerite have a fairly uniform size of 10 to 15 μm, and they yield compositions very close to theoretical, with no significant substitutions; the Zn content shown in Table 3 comes probably from the enclosing sphalerite. However, chalcopyrite was not observed in the tiny dispersed granules of sphalerite mentioned above.

The muscovite + phosphate veins (II)

Muscovite is greenish in hand specimens. It occurs in a dominant very fine-flaked form (50 to 400 μm, Fig. 4),

Table 2. Chemical composition of zircon and uraninite. Zircon normalized to 4 oxygen atoms *pfu*, uraninite to 2 oxygen atoms *pfu*.

	Zircon				Uraninite
	1	2	x̄(6)	σ	K-1
P_2O_5	0.32	0.98	0.38	0.34	0.14
SiO_2	31.62	31.52	32.32	0.75	0.03
ZrO_2	60.52	60.67	61.27	1.76	0.09
HfO_2	4.63	5.03	4.95	0.19	0.00
ThO_2	0.18	0.00	0.05	0.08	0.99
UO_2	1.52	0.58	1.04	1.09	91.64
Al_2O_3	0.05	0.04	0.03	0.02	0.03
Sc_2O_3	0.25	0.00	0.07	0.10	0.00
CaO	0.00	0.54	0.13	0.23	0.11
FeO	0.23	1.07	0.31	0.43	0.01
PbO	0.15	0.29	0.17	0.14	5.93
Total	99.47	100.72	100.72		98.97
	atoms per formula unit				
P	0.009	0.026	0.010	0.009	0.005
Si	0.996	0.977	1.001	0.019	0.001
ΣT	1.005	1.003	1.011		
Zr	0.930	0.917	0.926	0.021	0.002
Hf	0.042	0.045	0.044	0.001	0.000
Th	0.001	0.000	0.000	0.000	0.010
U	0.011	0.004	0.007	0.008	0.939
Al	0.002	0.001	0.001	0.001	0.002
Sc	0.007	0.000	0.002	0.003	0.000
Ca	0.000	0.018	0.004	0.008	0.005
Fe	0.006	0.028	0.008	0.011	0.000
Pb	0.001	0.002	0.001	0.001	0.073
ΣA	1.000	1.015	0.994		

Table 3. Chemical composition of sphalerite and chalcopyrite. Sphalerite normalized to the sum of 2 atoms *pfu*, chalcopyrite to 4 atoms *pfu*.

	Coarse sphalerite			Fine-grained sphalerite			Chalcopyrite
	1A–1	1A–2	1A–3	1B–3	1C–2	1C–1	1A–Inc
Zn	65.06	64.99	65.02	63.33	62.79	62.93	2.23
Fe	2.01	2.33	2.47	2.72	2.88	3.29	29.26
Mn	0.03	0.04	0.03	0.72	1.08	1.13	0.01
Cd	0.37	0.62	0.61	0.35	0.37	0.34	0.00
Cu	0.14	0.03	0.04	0.16	0.00	0.28	33.45
As	0.00	0.00	0.02	0.04	0.04	0.00	0.02
Sb	0.05	0.03	0.00	0.00	0.02	0.06	0.02
Sn	0.00	0.00	0.01	0.00	0.00	0.00	0.01
S	33.12	33.11	33.15	32.72	32.67	32.63	35.10
Total	100.77	101.15	101.34	100.04	99.86	100.66	100.10
	atoms per formula unit						
Zn	0.961	0.958	0.957	0.942	0.935	0.931	0.063
Fe	0.035	0.040	0.043	0.047	0.050	0.057	0.962
Mn	0.000	0.001	0.000	0.013	0.019	0.020	0.000
Cd	0.003	0.005	0.005	0.003	0.003	0.003	0.000
Cu	0.002	0.000	0.001	0.002	0.000	0.004	0.966
As	0.000	0.000	0.000	0.001	0.001	0.000	0.000
Sb	0.000	0.000	0.000	0.000	0.000	0.001	0.000
Sn	0.000	0.000	0.000	0.000	0.000	0.000	0.000
Σ *cat*	1.001	1.004	1.006	1.008	1.008	1.016	1.992
S	0.998	0.995	0.994	0.992	0.992	0.984	2.008

and in distinctly larger, albeit still rather small flakes (0.5–2 mm). The chemical composition of both size fractions, analyzed by electron microprobe, is about the same, corresponding to $(K_{0.90}Na_{0.06})_{\Sigma 0.96}(Al_{1.86}Fe^{2+}_{0.12}Mg_{0.03})_{\Sigma 2.01}(Si_{3.10}Al_{0.90})_{\Sigma 4.00}O_{20}(OH)_4$, with mere traces of Rb and Cl, and F below detection limit. The well-balanced dioctahedral formula suggests that Li and Fe^{3+} are present, if at all, in negligible amounts.

Triphylite, $Li(Fe>Mn)^{2+}(PO_4)$, forms small subrectangular blocks, 0.1 to 0.3 mm long, which form comb-textured rims separating the muscovite-phosphate veins from the wolfeite masses. In hand specimens, triphylite is tarnished rusty brown by slight incipient oxidation, and darkened deep grey by microscopic veining by alluaudite, hagendorfite and UK-D (Fig. 5). Wolfeite also replaces triphylite (Figs 5, 6), as does, locally, samuelsonite? (Fig. 4). Chemical composition of triphylite is relatively constant, with average value of Mn/(Mn+Fe)(at.) of 0.31 and a relatively high Mg/(Mg+Fe)(at.) of 0.11. In compositions normalized to 4 oxygen atoms and complemented by 1 Li *pfu*, Mg constitutes 6 to 9% of the *B*-site population (Table 4). The presence of Si is negligible but persistent at slightly less than 1 % of the *T*-site,

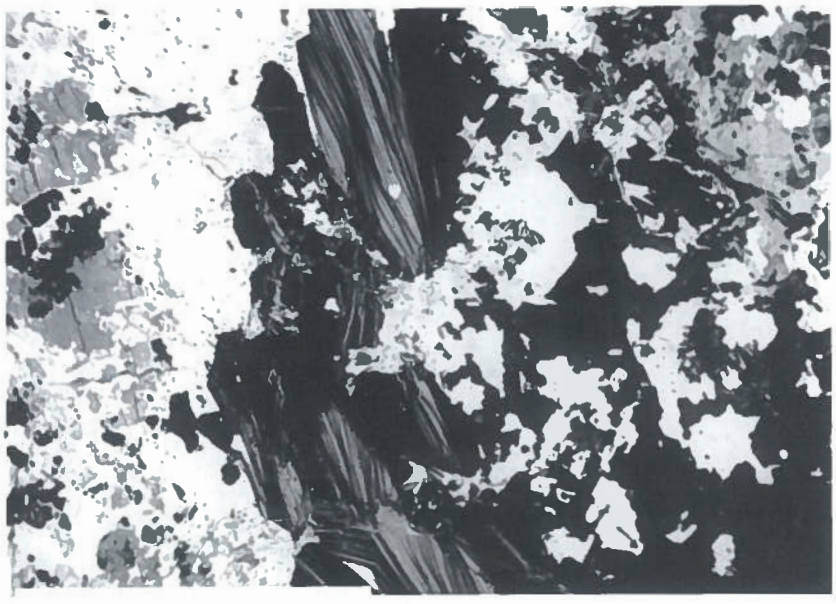

Fig. 4. Muscovite border (subvertical, foliated in center) of the fine-grained metasomatic assemblage of lazulite-scorzalite and quartz (black, undistinguished) with samuelsonite and relicts of arrojadite-dickinsonite (both white, undistinguished) to the right, and relicts of outer rim of triphylite (pale grey) replaced by samuelsonite (white), to the left. Scale bar is 500 μm long.

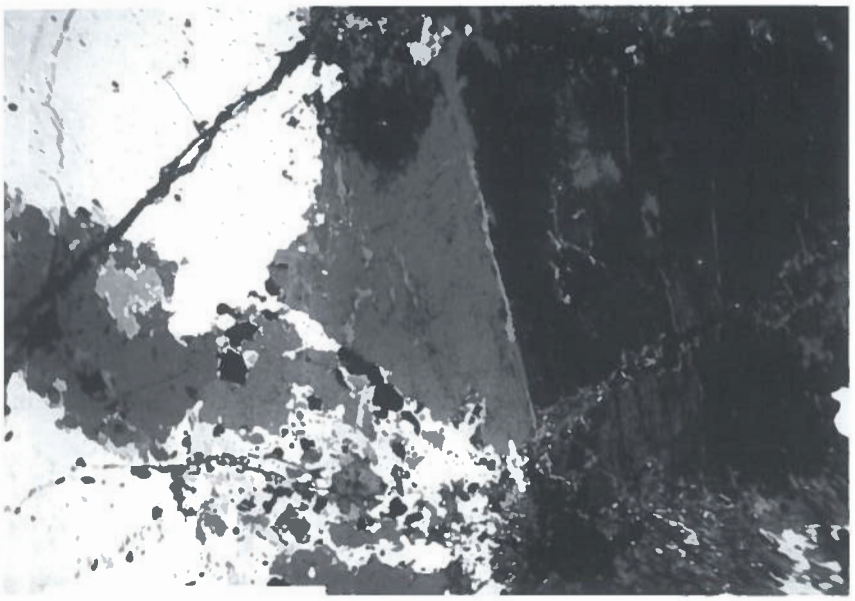

Fig. 5. Triphylite (medium grey, center to left) replaced by wolfeite (white), UK–D (pale grey grain, left of center), alluaudite (pale-grey veinlets, center), hagendorfite, ludlamite and chlorite? (all dark-grey to black on the right side). Scale bar is 500 μm long.

and the contents of Ca and Zn also are negligible. The contents of Al, Sr, Ba, Na, K, F and Cl are below the detection limits. Besides the good fit of the chemical composition, the identity of triphylite was also confirmed by X-ray powder diffraction; unit-cell refinement yielded *a* 6.033(4), *b* 10.359(4), *c* 4.705(2) Å, *V* 294.05(17) Å^3. The values of *a* and *b* are in reasonable agreement with *a* and *b* calculated for average composition (Table 4) using the equations of Fransolet et al. (1984; *a* 6.025, *b* 10.350, *c* 4.731 Å), but $c_{meas.}$ is much lower than the calculated value.

Lazulite-scorzalite, $(Mg,Fe)Al_2(PO_4)_2(OH)_2$, bright blue in hand specimens (Fig. 1) is a widespread member of the internal assemblage of the muscovite-phosphate veins, forming networks of interconnected platy grains up to 0.5 mm in aggregate size (Fig. 7). The composition of this phase is variable, as betrayed by variable brightness in BSE images (Fig. 8). Values of the Mg/(Mg+Fe) ratio vary from 0.73 to 0.43, but only a single composition falls into the range of scorzalite below 0.50; all others and the overall average have Mg>Fe of lazulite proper (Table 4). The contents of Si, Mn and Ca are variable but low, and those of Sr, Ba, Na, K, F and Cl are below the detection limits. X-ray powder diffration pattern of this phase was heavily affected by the presence of inevitable admixtures, but attempts at unit-cell refinement gave acceptable results which should correspond to the average chemical composition shown in Table 4: *a* 7,148(4), *b* 7,284(5), *c* 7.238(5) Å, *β* 120°31(4)', *V* 324.64(28) Å^3.

Samuelsonite?, $(Ca>Ba)Ca_8(Fe,Mn)^{2+}{}_4Al_2(PO_4)_{10}(OH)_2$, seems to be as widespread as lazulite-scorzalite in the vein interior, commonly closely associated with it, and also forming interconnected granular networks of about the same size (Fig. 7). However, its chemical composition is much more constant (Table 5). Chemical com-

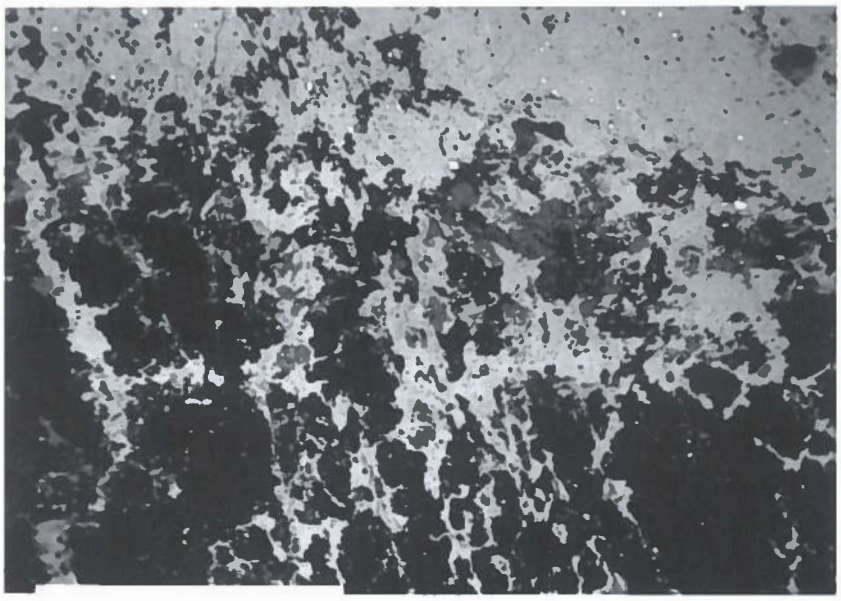

Fig. 6. Triphylite (black, bottom) replaced by wolfeite (pale grey, top) and hagendorfite (dark-grey patches associated with wolfeite, center). Scale bar is 500 μm long.

Table 4. Chemical composition of triphylite, normalized to 4 oxygen atoms + 1Li and lazulite-scorzalite, normalized to 8 oxygen atoms + 2(OH); † = calculated.

	Triphylite					Lazulite-scorzalite			
	39	73	x̄(8)	σ		49	92	x̄(9)	σ
P_2O_5	45.44	45.88	45.70	0.20	P_2O_5	44.38	44.78	44.93	0.71
SiO_2	0.30	0.32	0.28	0.05	SiO_2	0.16	0.03	0.09	0.09
MgO	2.03	2.22	2.11	0.22	Al_2O_3	32.21	31.02	31.06	0.59
CaO	0.00	0.00	0.01	0.01	MgO	9.72	5.44	7.40	1.50
MnO	13.62	12.24	13.16	0.75	CaO	0.03	0.04	0.02	0.02
FeO	29.72	30.23	30.07	0.58	MnO	0.19	0.38	0.28	0.07
$Li_2O^†$	9.68	9.71	9.72	0.03	FeO	6.24	12.88	9.85	2.10
Total	100.79	100.60	101.06		ZnO	0.00	0.02	0.01	0.01
					$H_2O^†$	5.70	5.63	5.65	0.07
					Total	98.63	100.22	99.29	
				atoms per formula unit					
P	0.989	0.994	0.990	0.004	P	1.976	2.020	2.017	0.018
Si	0.008	0.008	0.007	0.001	Si	0.008	0.002	0.005	0.005
Σ	0.997	1.002	0.998		Σ	1.984	2.022	2.022	
Mg	0.078	0.085	0.081	0.008	Al	1.997	1.948	1.941	0.038
Ca	0.000	0.000	0.000	0.000					
Mn	0.296	0.265	0.285	0.016	Mg	0.762	0.432	0.584	0.112
Fe	0.639	0.647	0.644	0.012	Ca	0.002	0.002	0.001	0.001
Σ	1.013	0.997	1.010		Mn	0.008	0.017	0.013	0.003
					Fe	0.275	0.574	0.438	0.097
Li	1.000	1.000	1.000		Zn	0.000	0.001	0.000	0.000
					Σ	1.047	1.025	1.036	
					OH	2.000	2.000	2.000	

position reasonably matches the formula of samuelsonite as generalized from structure refinement (Moore et al. 1975) but with three exceptions: the wt. % totals are slightly lower than desirable (by 1 to 2 %), Ba is below or at the detection limit, and the cations normalized to 42 anions *pfu* show a surplus of Mn which is close to the deficit in the bulk of the two Ca sites. However, the same deviations in Ca and Mn were also detected in the electron-microprobe and wet-chemical analyses of type material (Moore et al. 1975), and in those of samuelsonite from Buranga (Fransolet et al. 1992); the latter showed BaO locally as low as 0.89 wt. %. The substitution of Mn for Ca is known operate in minerals in general (*e. g.*, axinite), and in phosphates in particular (*e. g.*, graftonite-beusite); thus this substitution may be considered a real possibility in samuelsonite. In case our mineral is not samuelsonite, it would correspond to a new species with the condensed formula very close to $(Ca>>Na)_8$ $(Mn>Fe>>Mg)_5$ Al_2 $(PO_4)_{10}(OH)_2$, possibly with minor Li.

Eosphorite, $(Mn>Fe)^{2+}AlPO_4(OH)_2.H_2O$, forms scattered grains 20 to 40 μm across, associated with lazulite-scorzalite (Fig. 8). Eosphorite could not be verified by X-ray diffraction but the chemical composition, normalized to 5 oxygen atoms + 2(OH), leaves no doubt about its identity (Table 5). The values of Mn/(Mn+Fe)(at.) are variable within rather narrow limits, 0.64 to 0.70, distinctly above the childrenite minimum. The contents of Mg, Ca and Sr are minor, Si, Zn, Ba, Na, K, F and Cl are below detection limits.

Montebrasite, $LiAlPO_4(OH)$, forms rare isolated grains about 50 μm across, associated with lazulite-scorzalite and samuelsonite. Electron-microprobe analysis detected substantial Al and P, and traces of Fe, Mn, Ca, Mg and Si; fluorine was below the detection limit. Normalization to 4 oxygen atoms + (OH) with 1 Li *pfu* generated montebrasite formula but with significant deviations from integral values for Al (–6 % relative) and P (+4 % relative). Slight alteration may be the reason.

Calcite was identified optically and by a qualitative EDS examination as scattered 5 to 30 μm grains in the muscovite + phosphate matrix of the veins.

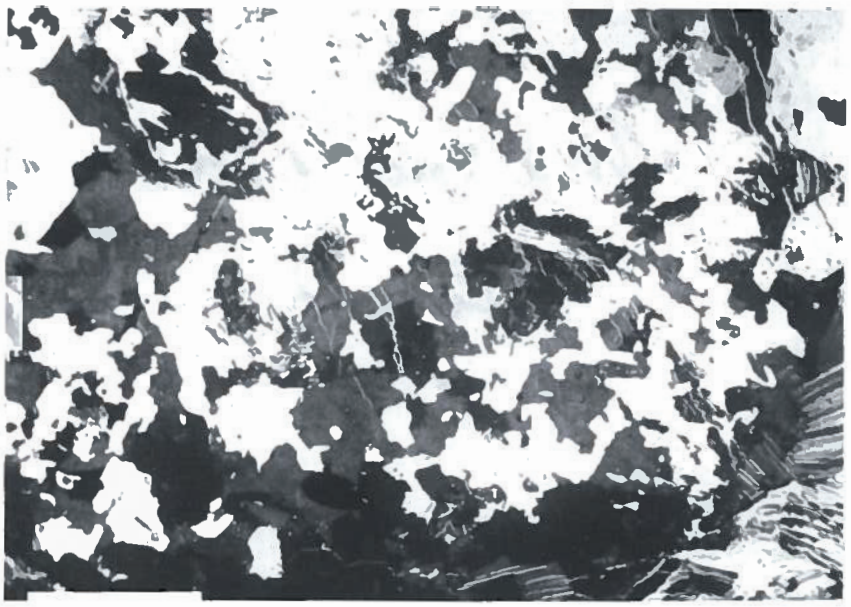

Fig. 7. Lazulite-scorzalite (variable medium grey) intergrown with samuelsonite? containing relicts of arrojadite-dickinsonite (all white, undistinguished); quartz (black) at the bottom, very fine veinlets of fairfieldite? (white) crosscut all of the above minerals. Scale bar is 200 μm long.

Table 5. Chemical composition of samuelsonite?, normalized to 40 oxygen atoms + 2(OH) and with cations assigned by structural allocation of species, and * with surplus of Mn compensating bulk deficit in the two Ca sites; eosphorite, normalized to 5 oxygen atoms + 2(OH) + (H2O). † = calculated; – = absent.

	Samuelsonite?			Samuelsonite?				Eosphorite	
	50	x̄(4)	σ	50*	x̄(4)*	σ*		84	86
P_2O_5	42.45	42.62	0.45	42.45	42.62	0.45	P_2O_5	31.30	30.98
Al_2O_3	6.29	6.12	0.17	6.29	6.12	0.17	Al_2O_3	21.84	21.68
MgO	0.20	0.17	0.05	0.20	0.17	0.05	MgO	0.16	0.07
CaO	26.68	27.10	0.34	26.68	27.10	0.34	CaO	0.20	0.12
MnO	10.73	10.81	0.57	10.73	10.81	0.57	MnO	18.51	20.95
FeO	9.59	9.23	0.33	9.59	9.23	0.33	FeO	10.60	9.00
SrO	0.00	0.02	0.02	0.00	0.02	0.02	SrO	0.05	0.04
Na_2O	0.37	0.23	0.11	0.37	0.23	0.11	$H_2O^†$	15.58	15.52
K_2O	0.02	0.01	0.01	0.02	0.01	0.01	Total	98.24	98.36
$H_2O^†$	1.08	1.08	0.01	1.08	1.08	0.01			
Total	97.41	97.37		97.41	97.37				
				atoms per formula unit					
P	10.001	10.036	0.031	10.001	10.036	0.031	P	1.020	1.013
Al	2.063	2.007	0.046	2.063	2.007	0.046	Al	0.991	0.987
Ca	7.955	8.076	0.124	7.955	8.076	0.124	Mg	0.009	0.004
Mn	–	–	–	0.844	0.760	0.085	Ca	0.008	0.005
Sr	0.000	0.003	0.004	0.000	0.003	0.004	Mn	0.604	0.686
K	0.007	0.003	0.003	0.007	0.003	0.003	Fe	0.341	0.291
Na	0.200	0.121	0.058	0.200	0.121	0.058	Sr	0.001	0.001
Σ	8.162	8.203		9.006	8.963		Σ	0.963	0.987
Mg	0.083	0.069	0.022	0.083	0.069	0.022	OH	2.000	2.000
Fe	2.232	2.146	0.083	2.232	2.146	0.083			
Mn	2.529	2.545	0.130	1.685	1.786	0.096	H_2O	1.000	1.000
Σ	4.844	4.760		4.000	4.000				
OH	2.000	2.000		2.000	2.000				

The metasomatic wolfeite assemblage (III)

Wolfeite, $(Fe>Mn)^{2+}_2(PO_4)(OH)$, composes randomly oriented, subhedral, stubby prismatic crystals, milk-chocolate in colour. The individual crystals range from 10 to 150 μm in length (Fig. 9). Poor but distinct cleavages are indicated parallel to the elongation of the prisms. Fine-grained wolfeite replaces, and encloses relicts of arrojadite-dickinsonite and triphylite (Figs 2, 3, 5, 6, 11). In polarizing microscope, wolfeite is very pale brown with negligible pleochroism. Refractive indices are α 1.741, β 1.743, γ 1.746, $\gamma - \alpha$ 0.005; calculation yields (+)2V of 37°.

X-ray powder diffraction pattern of the Otov I wolfeite is in good agreement with that of wolfeite from the Palermo pegmatite, North Groton, New Hampshire (Frondel 1949) and with the pattern presented by Antenucci et al. (1989), which was used for indexing selected diffractions in our cell refinement. Unit-cell dimensions of the Otov I wolfeite are a 12.327(3), b 13.225(3), c 9.845(2) Å, β 108°23(1)', V 1522.95(47) Å^3.

Chemical composition (Table 6) corresponds to wolfeite with Mn/(Mn+Fe)(at.) slightly variable about the average value of 0.46. The Mg content is subordinate, the Mg/(Mg+Fe) ratio (at.) varies from 0.10 to 0.05. The contents of Na, K, Ca, Zn, Sr, Ba, Si, Al, F and Cl are negligible, and generally below the quantitatively meaningful detection level. Average of 27 analyzed spots, normalized to 5 anions, leads to the formula of $(Fe_{1.060}Mn_{0.846}Mg_{0.075}Ca_{0.004}Zn_{0.003})_{\Sigma 1.989}P_{1.004}(OH_{0.997}F_{0.003})_{\Sigma 1.000}$. Dark-brown patches in the otherwise pale-brown fresh wolfeite (Fig. 1) are most probably caused by incipient oxidation. Chemical composition of these patches varies from normal to slightly cation-deficient, and the unit-cell refinement yields values slightly different from those

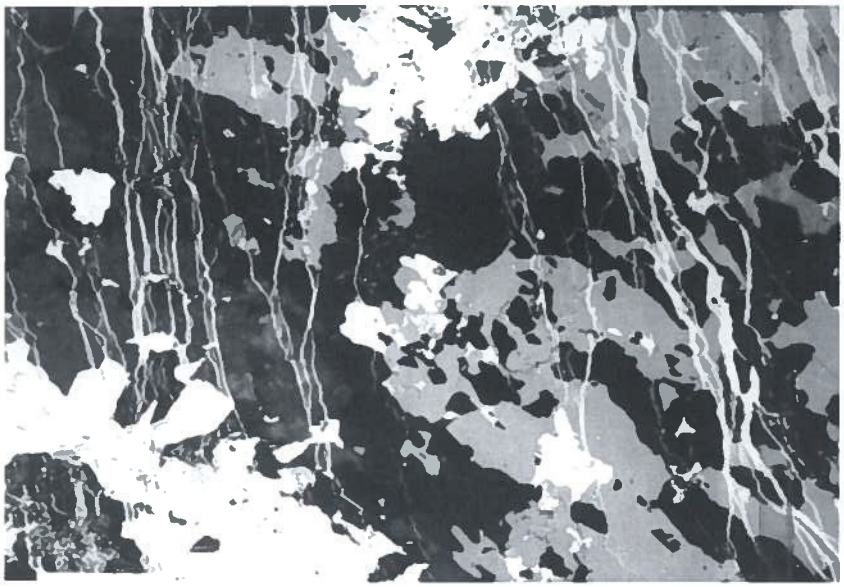

Fig. 8. Lazulite-scorzalite (mottled grey to black) intergrown with samuelsonite? (off-white, lower left), eosphorite (pale grey) and relics of arrojadite-dickinsonite (white, top center), veined by fairfieldite? (white, subvertical) Scale bar is 200 μm long.

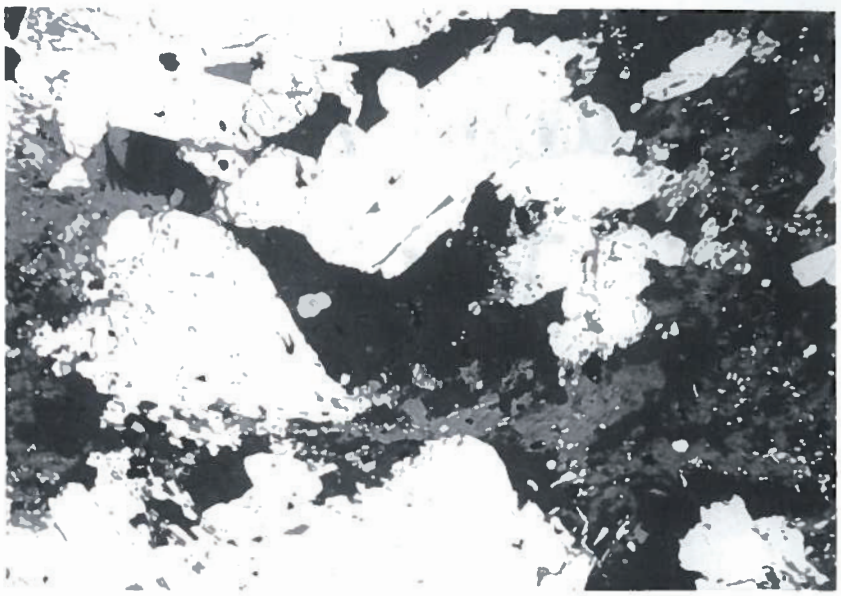

Fig. 9. Subhedral crystals of wolfeite (white) with interstices filled by F-bearing hydroxylapatite (blackish grey), and both in part replaced by Mn, Fe-rich hydroxylchlorapatite (pale grey). Scale bar is 200 μm long.

quoted above, with much greater standard deviations: *a* 12.321(5), *b* 13.223(7), *c* 9.845(4) Å, *β* 108°25(2)', *V* 1521.79(93) Å³.

Fluorine-bearing manganoan *hydroxylapatite* mainly fills interstices among aggregates of wolfeite (Fig. 9); replacement of wolfeite and occurrences of late cross-cutting veinlet in wolfeite are rare. Virtual absence of Si and Al, and negligible Sr and Ba, characterize this hydroxylapatite (Table 6).

Alluaudite, $Na_4(Na,Ca,Mn^{2+},\square)_4 Mn^{2+}{}_4(Fe^{3+}>Fe^{2+},Mg,Mn^{2+})_8 (PO_4)_{12}$, is found as rare microveinlets penetrating and replacing triphylite (Figs 5, 11). Negligible dimensions, 3 to 10 μm, prevent identification by X-ray diffraction but the results of chemical analysis are unmistakable (Table 7): recalculation of the composition on the basis of 48 oxygens + 12 P *puc* (Moore – Ito 1979) leading to partial conversion of Fe^{2+} to Fe^{3+} leads to good formulas indicative of "Al-free" alluaudite dominant over a subordinate hagendorfite component, strongly Na-dominant over Ca but with substantial vacancies in the *B* site. The contents of Si, Sr, Ba and K are negligible, but Mg is a prominent substituent for $(Fe,Mn)^{2+}$.

Table 6. Chemical composition of wolfeite, normalized to 4 oxygen atoms + 1(OH, F), hydroxylapatite and hydroxylchlorapatite, normalized to 12 oxygen atoms + 1(OH, F, Cl); † = calculated.

	Wolfeite						Hydroxyl-apatite		Hydroxyl-chlorapatite	
	14	37	44	x̄(27)	σ		x̄(6)	σ	x̄(4)	σ
P_2O_5	32.04	32.01	32.40	32.15	0.35	P_2O_5	41.88	0.45	40.28	0.80
MgO	1.45	2.35	1.07	1.37	0.27	SiO_2	0.00	0.00	0.14	0.29
CaO	0.06	0.03	0.50	0.10	0.16	Al_2O_3	0.01	0.01	0.02	0.04
MnO	26.84	21.19	29.93	27.07	2.04	CaO	52.32	1.60	43.16	1.61
FeO	34.99	38.97	31.19	34.35	1.73	MnO	3.77	1.39	11.06	1.26
ZnO	0.02	0.91	0.19	0.12	0.23	FeO	0.36	0.28	1.89	1.24
F	0.00	0.23	0.03	0.02	0.05	ZnO	0.03	0.05	0.03	0.06
H_2O†	4.07	3.97	4.06	4.05	0.03	SrO	0.01	0.01	0.44	0.45
O=F	0.00	-0.10	-0.01	-0.01	0.02	BaO	0.06	0.05	0.03	0.04
Total	99.47	99.56	99.36	99.22		Na_2O	0.01	0.02	0.01	0.02
						F	0.60	0.28	0.08	0.07
						Cl	0.01	0.01	3.02	0.33
						H_2O†	1.49	0.14	0.91	0.06
						O=F	-0.26	-0.12	-0.03	0.03
						O=Cl	0.00	0.00	-0.68	0.08
						Total	100.29		100.36	
						atoms per formula unit				
P	1.000	0.996	1.009	1.004	0.006	P	2.989	0.012	2.979	0.034
						Si	0.000	0.000	0.013	0.025
Mg	0.080	0.129	0.059	0.075	0.015	Al	0.001	0.001	0.002	0.004
Ca	0.002	0.001	0.020	0.004	0.006	Σ	2.990		2.994	
Mn	0.838	0.659	0.933	0.846	0.065					
Fe	1.079	1.197	0.960	1.060	0.052	Ca	4.726	0.114	4.040	0.122
Zn	0.001	0.025	0.005	0.003	0.006	Mn	0.270	0.101	0.819	0.098
Σ	2.000	2.011	1.977	1.989		Fe	0.026	0.020	0.139	0.092
						Zn	0.002	0.003	0.002	0.004
F	0.000	0.027	0.003	0.003	0.005	Sr	0.000	0.001	0.022	0.022
OH	1.000	0.973	0.997	0.997	0.005	Ba	0.002	0.002	0.001	0.001
Σ	1.000	1.000	1.000	1.000		Na	0.002	0.004	0.001	0.003
						Σ	5.027		5.024	
						F	0.161	0.076	0.022	0.020
						Cl	0.001	0.001	0.447	0.051
						OH	0.838	0.076	0.531	0.033
						Σ	1.000		1.000	

Hagendorfite, $Na_4(Na,Ca,Mn^{2+},\square)_4Mn^{2+}{}_4(Fe^{2+}>Fe^{3+},Mg,Mn^{2+})_8(PO_4)_{12}$, is found in the same association, form and size as alluaudite, evidently also a replacement product of triphylite. Locally it is closely associated with wolfeite which replaces triphylite (Fig. 6). In contrast to alluaudite, however, hagendorfite contains substantial Al (Table 7). Aluminum was considered basically absent from the alluaudite-group minerals (Moore – Ito 1979). However, Fransolet et al. (1995) collected ample evidence for the existence of Al-bearing alluaudite which bridges the alleged compositional gap between the "Al-free" alluaudite group and the "4 Al *puc*" wyllieite group. The structural affiliation of these compositionally transitional phases is, however, still uncertain.

UK-D is an unknown phase which also participates in replacement of triphylite in the form of irregular grains or microgranular aggregates ~50 μm across (Fig. 5).

Table 7. Chemical composition of alluadite and hagendorfite, normalized to 48 oxygen atoms and 12P; † = calculated, – = absent.

	Alluaudite		Hagendorfite	
	38	82	36	65
P_2O_5	44.28	43.64	44.58	44.69
SiO_2	0.21	0.02	0.00	0.27
Al_2O_3	0.00	0.00	5.90	3.26
Fe_2O_3†	19.61	20.27	4.43	10.36
MgO	1.79	1.26	2.66	3.01
CaO	0.26	0.88	1.14	0.33
MnO	14.43	14.29	19.96	17.88
FeO	11.30	9.25	13.40	11.70
ZnO	0.00	0.02	0.01	0.00
SrO	0.02	0.01	0.00	0.02
BaO	0.02	0.03	0.00	0.02
Na_2O	9.32	10.07	8.07	9.25
K_2O	0.01	0.04	0.01	0.00
Total	101.24	99.78	100.17	100.78
	atoms per formula unit			
P	12.000	12.000	12.000	12.000
Si	0.067	0.006	0.000	0.086
ΣT	12.067	12.006	12.000	12.086
Na	4.000	4.000	4.000	4.000
Ca	0.000	0.000	0.000	0.000
ΣA	4.000	4.000	4.000	4.000
Na	1.784	2.342	1.980	1.688
Ca	0.089	0.306	0.388	0.112
Sr	0.003	0.002	0.000	0.004
Ba	0.004	0.004	0.000	0.002
K	0.004	0.017	0.004	0.000
Mn	0.515	–	1.474	1.022
•	1.601	1.329	0.154	1.172
ΣB	4.000	4.000	4.000	4.000
Mg	0.602	0.082	0.000	0.000
Mn	3.398	3.931	3.901	3.781
Fe	–	–	0.099	0.219
ΣC	4.000	4.013	4.000	4.000
Fe^{3+}	4.724	4.955	1.061	2.472
Al	0.000	0.000	2.211	1.219
Fe^{2+}	3.024	2.512	3.465	2.884
Zn	0.000	0.005	0.002	0.000
Mg	0.252	0.528	1.261	1.423
Mn	–	–	–	–
ΣD	8.000	8.000	8.000	7.998

Table 8. Chemical composition of UK–D, normalized to 2P + $1H_2O$ and 2P + Li(OH), and ludlamite normalized to 2P + $4H_2O$; † = calculated, – = absent.

	UK-D, $1H_2O$		UK-D, Li(OH)			Ludlamite	
	35	48	35	48		$\bar{x}(9)$	σ
P_2O_5	39.38	39.62	39.38	39.62	P_2O_5	30.39	0.46
Al_2O_3	0.04	0.01	0.04	0.01	SiO_2	0.16	0.31
MgO	0.49	0.58	0.49	0.58	MgO	0.39	0.28
FeO	13.50	13.39	13.50	13.39	FeO	33.30	0.77
MnO	23.50	24.11	23.50	24.11	MnO	10.99	0.91
ZnO	0.01	0.00	0.01	0.00	ZnO	0.35	0.23
CaO	16.14	15.60	16.14	15.60	CaO	0.04	0.05
SrO	0.42	0.51	0.42	0.51	SrO	0.02	0.02
BaO	0.02	0.02	0.02	0.02	BaO	0.02	0.03
Li_2O†	–	–	4.15	4.17	K_2O	0.01	0.01
Na_2O	0.03	0.04	0.03	0.04	H_2O†	15.43	0.23
K_2O	0.01	0.01	0.01	0.01	Total	91.09	
H_2O†	5.00	5.03	2.50	2.51			
Total	98.54	98.93	100.18	100.58			
	atoms per 2P						
P	2.000	2.000	2.000	2.000	P	2.000	0.000
					Si	0.012	0.024
Al	0.003	0.001	0.003	0.001	Σ	2.012	
Mg	0.044	0.052	0.044	0.052			
Fe	0.677	0.668	0.677	0.668	Mg	0.045	0.032
Mn	1.194	1.218	1.194	1.218	Fe	2.165	0.060
Zn	0.000	0.000	0.000	0.000	Mn	0.724	0.058
Σ	1.918	1.939	1.918	1.939	Zn	0.020	0.013
					Ca	0.004	0.004
Ca	1.037	0.997	1.037	0.997	Sr	0.001	0.001
Sr	0.015	0.018	0.015	0.018	Ba	0.001	0.001
Ba	0.000	0.000	0.000	0.000	K	0.001	0.001
Σ	1.052	1.015	1.052	1.015	Σ	2.960	
Na	0.003	0.005	0.003	0.005	H_2O	4.000	4.000
K	0.001	0.001	0.001	0.001			
Σ	0.004	0.006	0.004	0.006			
Li	–	–	1.000	1.000			
OH	–	–	1.000	1.000			
H_2O	1.000	1.000	–	–			

Normalization of the EMPA-established composition to 2P or 8 oxygen equivalents leads to $(Ca»Sr)(Mn>Fe^{2+}»Mg)_2(PO_4)_2$. This formula is, however, incomplete as the analysis yielded a total of only 93.5 to 94 wt. %. The complement to ~100 wt. % can be achieved by adding either 1 H_2O, or Li + (OH) to the formula (Table 8). Both options seem to be geochemically and paragenetically feasible, but neither of them resembles any established mineral. However, P. Keller (pers. comm. 2000) encountered a compositionally similar phase in granitic pegmatites of Namibia.

Late veining and replacement (IV)

Ludlamite, $(Fe>Mn)_3(PO_4)_2 \cdot 4H_2O$, composes locally irregular grains but mainly thin veinlets, 5 to 25 μm across, which replace and crosscut virtually all other phosphates (Figs 3, 10, 11). X-ray diffraction is not possible on this mineral. Chemical composition gives the atomic ratio of (Fe,Mn):P as 3:2, but the remainder to 100 wt. % in the analytical results is consistently much greater than that

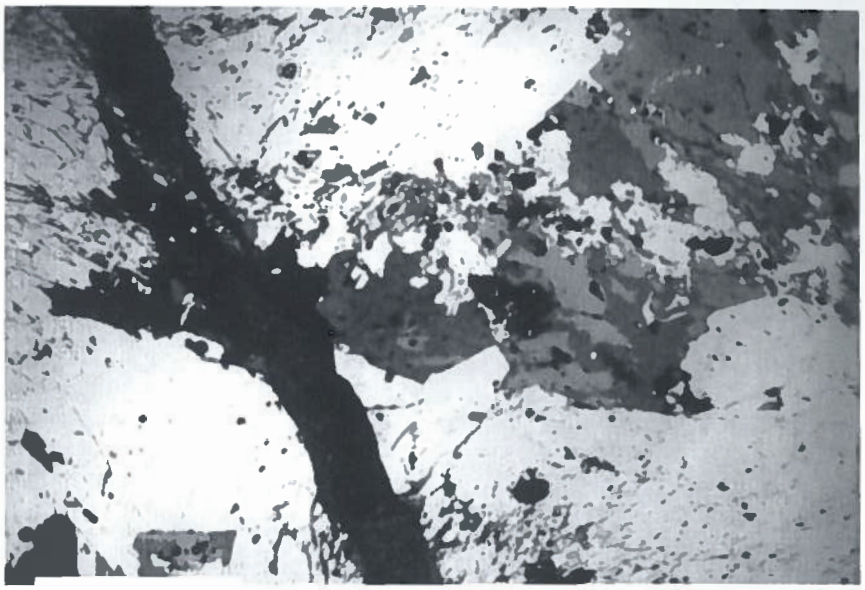

Fig. 10. Veinlet of ludlamite with goyazite (black, undistinguished) crosscutting wolfeite (off-white) with relicts of arrojadite-dickinsonite (pale grey, right of center), which is in part replaced by hydroxylapatite (medium grey). Scale bar is 200 μm long.

required by the ludlamite formula $Fe^{2+}_3(PO_4)_2{\cdot}4\,H_2O$ (Table 8). The best fit is obtained with 6 H_2O, which does not correspond to any known mineral. In contrast, 7 H_2O as in the (Mn>Fe)-bearing switzerite and 8 H_2O as in the (Fe»Mn)-bearing vivianite lead to very excessive wt. % totals. Ludlamite remains the most probable (albeit not guaranteed) possibility, as the grains and veinlets of our mineral commonly show considerable variations in brightness on BSE images, despite virtually constant values of the $FeO:MnO:P_2O_5$ *ratio* but with somewhat variable *sum* of these oxides. This suggests microporosity in this mineral, largely below the resolution power of EMPA but locally observed at near-maximum magnification in BSE images; such a microporosity might account for the ~8 to ~11 % remainder to the 100 wt. % total.

Goyazite, $SrAl_3(PO_4)_2(OH)_5{\cdot}H_2O$, is relatively widespread, commonly in the form of grains 10 to 40 μm across, which are attached to the ludlamite veinlets (Fig. 10) or participate directly in the veinlet filling. Verification by X-ray diffraction was not feasible but recalculation of the EMPA-established composition, based on 2 P + 7 H, generated a near-ideal match with the goyazite formula (Table 9). The only significant aberration is Si, which happens to compensate for the deficiency of *octahedral* Al. Improbable as it is structurally, such a substitution would fit the required stoichiometry. Additional analyses of other grains, mainly from the closely adjacent but incomplete phase association mentioned in the discussion, gave just traces of Si, but a slight deficiency in Al, and in the [(OH)+H_2O]-adjusted total which is low by ~2.5 wt. %.

Mn>Fe-rich *hydroxylchlorapatite* replaces wolfeite and hydroxylapatite (Fig. 9), and is rather abundant in late veinlets crisscrossing wolfeite and, in part, the muscovite + phosphate veins. Si, Al and Ba are locally enriched and Sr is persistently higher in the hydroxylchlo-

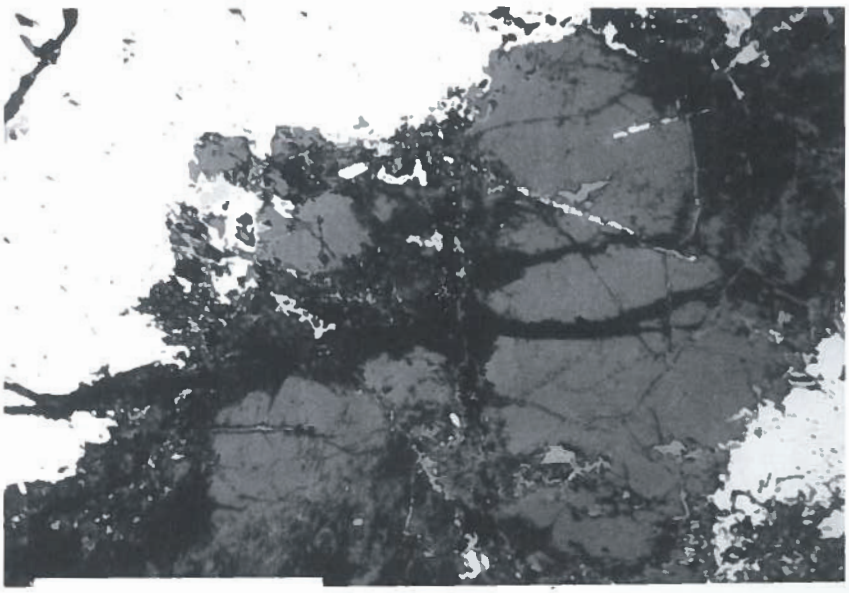

Fig. 11. Triphylite (medium grey) replaced by wolfeite (white areas) and alluaudite (white veinlets inside triphylite); ludlamite (black) veins and replaces triphylite but leaves alluaudite more or less intact (near center). Scale bar is 500 μm long.

Table 9. Chemical composition of goyazite and fairfieldite?, normalized to 2P + 5(OH) + 2H_2O, respectively; † = calculated.

Goyazite		Fairfieldite?	
P_2O_5	31.20	P_2O_5	36.95
SiO_2	1.75	Al_2O_3	0.88
Al_2O_3	31.81	MgO	0.21
FeO	0.11	FeO	5.62
MnO	0.06	MnO	11.97
ZnO	0.09	ZnO	0.07
CaO	1.55	CaO	28.03
SrO	18.91	BaO	0.11
Na_2O	0.22	Na_2O	0.12
H_2O†	13.86	H_2O†	9.38
Total	99.56	Total	93.34
atoms per formula unit			
P	2.000	P	2.000
Al	2.839	Mn	0.648
Si	0.133	Fe	0.300
Σ	2.972	Al	0.066
		Mg	0.020
Sr	0.830	Zn	0.003
Ca	0.126	Σ	1.037
Na	0.032		
Fe	0.007	Ca	1.920
Mn	0.004	Na	0.015
Σ	0.999	Ba	0.003
		Σ	1.938
OH	5.000		
		H_2O	2.000
H_2O	1.000		

rapatite relative to the hydroxylapatite discussed above (Table 6). Hydroxyl (calculated by normalization to 12 oxygen atoms + 1 [OH,F,Cl]) is systematically higher than Cl in hydroxylchlorapatite, but chlorine comes so close second that incorporation of both anions into the name is warranted: average value of Cl/(Cl+[OH])(at.) is 0.46.

Fairfieldite?, $Ca_2(Mn>Fe)(PO_4)_2 \cdot 2H_2O$, was encountered in the form of microscopic thin veinlets crosscutting earlier phosphates, including hydroxychlorapatite and chlorite? (Fig. 8). The identity of fairfieldite? must be considered somewhat questionable, as recalculation to the generally established formula gives a total of only ~93 wt. % (Table 9). A satisfactory wt. % total is generated assuming 3 instead of 2 H_2O, but no mineral is known at present which would correspond to $Ca_2(Mn,Fe)^{2+}(PO_4)_2 \cdot 3\ H_2O$. Possibly the same argument may apply to the low total yielded by the 2 H_2O formula as that forwarded for ludlamite, although microporosity was not observed in the BSE images. However, compositions perfectly fitting the theoretical formula of fairfieldite were obtained on well-defined crystals of this mineral from a closely adjacent phosphate association mentioned in the discussion below.

Chlorite? forms irregular microscopic clots and ragged veinlets associated with the late phosphates, particularly hydroxylchlorapatite. Dark green and strongly pleochroic, it could not be separated for X-ray diffraction study. The chemical composition normalized to 10 oxygen atoms and 8 (OH) gives the average formula of $(Fe^{2+}_{3.90}Al_{1.58}Mg_{0.26}Mn_{0.09}Ca_{0.02})_{\Sigma 5.85}(Si_{2.56}Al_{1.40}P_{0.04})_{\Sigma 4.00}O_{10}(OH)_8$, with traces of Zn, Na and F. This composition is close to that of chamosite or thuringite on one hand, and to that of the "septechlorite" berthierine on the other; hence the questionmark.

Discussion

With the exception of wolfeite, the properties of which are rather straightforward, the present study does not contribute much material to the crystal chemistry of pegmatite phosphates, as chemical composition is in most cases the sole well-defined characteristic, and is not accompanied by structural data. Desirable as additional studies would be in cases of, e. g., samuelsonite or UK-D, lack of suitable material does not allow expansion of our current research. Thus the discussion is focused on the paragenetic and geochemical aspects of the examined phosphates, as the chemistry of individual phases and their textural relationships provide ample material for this line of interpretation.

Paragenesis and geochemistry

(I) Arrojadite-dickinsonite is undoubtedly the oldest, primary phosphate, at the expense of which all later phases were formed. Generally known to form sizeable subhedral crystals associated with blocky K-feldspar, core quartz and book muscovite (Moore 1982), arrojadite-dickinsonite crystallizes at late magmatic temperatures (in our case of a P-enriched but generally Li- and B-poor pegmatite, ~500 °C). Arrojadite-dickinsonite fits the role of a primary precursor to other phosphates encountered here. In terms of cation contents, it is primarily a phosphate of Fe and Mn (~1:1) with subordinate Mg (Fig. 12), substantial Na, and minor K, Ca, Al (and probably Li). Association of primary pegmatite phosphates with sphalerite (and other sulphides, such as pyrrhotite, arsenopyrite) is well known from numerous localities worldwide (e. g., Hagendorf Süd, Bavaria, and Big Chief, South Dakota). Association of zircon with primary phosphates is not widespread, but it was noticed in the Otov I pegmatite by earlier authors (Čech 1981).

(II) The first replacement stage affecting arrojadite-dickinsonite is the formation of muscovite-rich veins, rimmed and intergrown by a series of OH-bearing phosphates of Li, Ca, Mg and Al (+ calcite). Fig. 12 shows the arrojadite-dickinsonite precursor surrounded by the metasomatic phases in qualitative terms, which do not, however, imply a quantitative relationship: Mg from the precursor phase certainly did not suffice for the formation of the rather abundant lazulite-scorzalite, and the Al content of the new assemblage could not be recruited solely from arrojadite-dickinsonite. The overall chemistry of the assemblage indicates influx of Mg, Al and Li from outside the original arrojadite-dickinsonite bodies under hydrous conditions. This event matches the metasomatic stage of Moore (1982), which generates dominantly hydroxylated phosphates in the approximate temperature range of 500 to 300 °C. The only exception to the "(OH)-only rule" is the eosphorite which contains

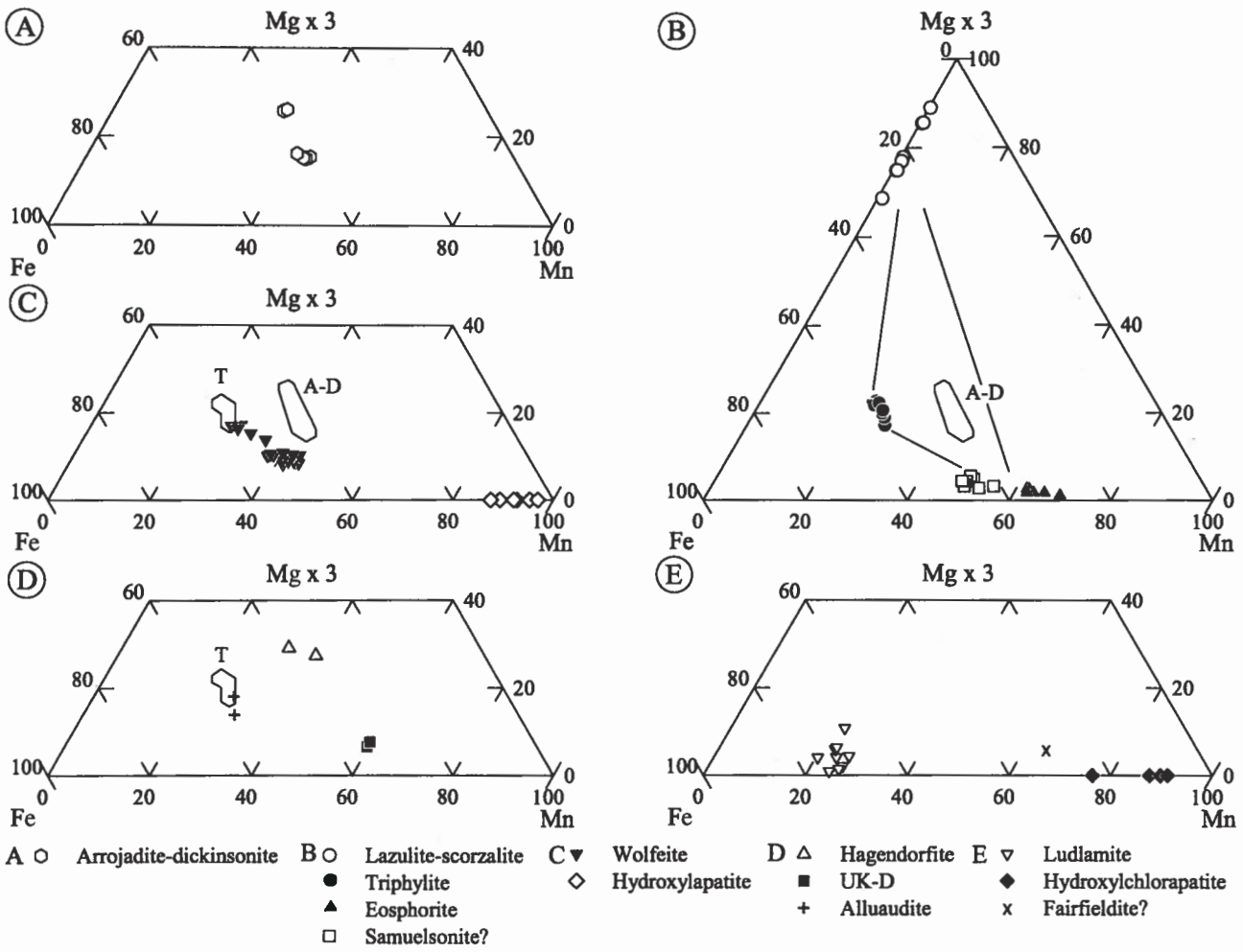

Fig. 12. The Fe – Mn – Mgx3 diagrams for (I) the primary arrojadite-dickinsonite (A), phosphates of the (II) muscovite + phosphate veins (B), the metasomatic (III) wolfeite assemblage (C) and the associated replacement products after triphylite (D), and for phases of (IV) the late veining and replacement (E). A–D – arrojadite-dickinsonite, T – triphylite.

molecular H_2O, but it is rare and its paragenetic position is somewhat uncertain.

(III) Relics of arrojadite-dickinsonite in wolfeite, and wolfeite replacing triphylite in rims of the muscovite + phosphate veins indicate that the third assemblage postdates the muscovite + phosphate veins. In contrast to the preceding process, this *en masse* replacement of arrojadite-dickinsonite by wolfeite + hydroxylapatite proceeded under conditions of partial cation leaching. The bulk of the wolfeite copies the Mn/(Mn+Fe) ratio of arrojadite-dickinsonite and triphylite (Fig. 12), but alkali metals and Al are removed. However, minor hydroxylapatite and traces of UK-D, both associated with wolfeite, may account for the released Ca.

Alluaudite and hagendorfite are always observed as outposts of the wolfeite metasomatism, penetrating triphylite; these two complex phosphates suggest perceptibly oxidizing conditions along the metasomatic front, as they are the only ones in the entire mineral suite which contain Fe^{3+}. Alluaudite mimics the triphylite value of Fe:Mn:Mg, but hagendorfite and UK-D are relatively enriched in Mn (Fig. 12).

(IV) The late phosphate assemblage penetrates, and in part replaces, all earlier phases. This assemblage fits the definition of secondary, H_2O-bearing phosphates of Moore (1982), which stabilize at or below ~200 °C. Most of the minerals identified here contain molecular H_2O, alone or in addition to (OH) groups, and all of them are exclusively Fe^{2+}-bearing.

In general, the primary arrojadite-dickinsonite sets the stage for the bulk Fe/Mn/Mg values of its alteration products, variable as they are individually because of their specific crystal-chemical preferences. The contents of Mg, Ca and Sr, combined with the scarcity of Ba, probably reflect contamination from the gabbroic host rock: either at the magmatic stage of crystallization of the primary phosphate, or in late fluids percolating the wallrock and the pegmatite, which gave rise to the secondary products. Chlorine is significantly present in some of the late phosphates, but F is remarkably low in the whole sequence, including muscovite, montebrasite and apatite. Similarly, subordinate Fe^{3+} is restricted to only a few minor phosphates: the entire phosphate assemblage is remarkably reduced.

Relationships to other phosphate assemblages

As indicated already in the introduction, the phosphate sequence examined here has escaped attention of previous authors, but it is far from being the only phosphate assemblage in the Otov I pegmatite. Graftonite-sarcopside intergrowths, blocky triphylite, apatite and montebrasite constitute quantitatively prominent primary phases. These primary phosphates suffered alteration processes, either relatively similar to those described here (muscovite veining with triphylite rims, Novotný 1956), or substantially different (e. g., strong leaching and oxidation generating voluminous ferrisicklerite and heterosite, Novotný 1956). It is impossible today to reconstruct the whole phosphate story in this pegmatite, as the spatial relations among the diverse primary phases and their alteration products were never sufficiently documented.

Even the history of the arrojadite-dickinsonite alteration presented here is incomplete, because the material examined is fragmentary. The left-hand side of the wolfeite slab shown in Fig. 1 consists of a part of a replacement assemblage, probably spreading from a fracture, comprised of coarse hydroxylapatite, samuelsonite?, muscovite, triphylite, hydroxylchlorapatite, goyazite, metaswitzerite?, fairfieldite, mitridatite ferroan rhodochrosite and two unknown phosphates: UK-G corresponding to Ca (Fe>Mn>Mg)$_5$(PO$_4$)$_4$·4 H$_2$O, and UK-H with the probable formula of Ca (Mn>Mg>Fe)$_5$Al$_3$(PO$_4$)$_6$(OH)$_3$·2 to 3 H$_2$O (both possibly with Li + OH). However, this association cannot be fitted into the overall scheme of arrojadite-dickinsonite breakdown without the study of adjacent material, which is not available.

Conclusions

Arrojadite-dickinsonite is added to the spectrum of primary magmatic phosphates in the Otov I pegmatite. In contrast to previous observations suggesting total resistance to replacements (Moore 1982), this arrojadite is extensively altered by two successive processes, and reduced to microscopic relics.

Wolfeite, considered a primary blocky phosphate with no documented cases of metasomatic origin (Plimer – Blucher 1979, Moore 1982), is shown here as the volumetrically main replacement product of arrojadite-dickinsonite. Maybe metasomatic claims of some early students of wolfeite (e. g., Frondel 1949) should not have been dismissed as unjustified.

Two stages of metasomatism affected the Otov I arrojadite-dickinsonite: (1) veining by muscovite and (OH)-bearing phosphates of Fe, Mn and largely imported Li, Ca, Mg and Al, under conditions preserving Fe (and consequently also Mn) in divalent state, followed by (2) massive replacement by mainly wolfeite, which largely preserves Mn/(Mn+Fe) but is preceded by partial oxidation of Fe in minor alluaudite and hagendorfite at the margin of metasomatic fronts.

Final alteration products comprise H$_2$O-, Cl- and (Fe,Mn)$^{2+}$-bearing, Sr-enriched phosphates which penetrate in limited quantities all of the preceding assemblages, and yet another incompletely preserved association of (OH)- and H$_2$O-bearing phosphates with ferroan rhodochrosite.

Arrojadite-dickinsonite and the sequence of its alteration products show remarkably low oxidation state and an extremely low F content. Enrichment in Ca, Mg and Sr, in the absence of any significant Ba, indicates contamination from the gabbroic wallrock.

Acknowledgements. This work was supported by Natural Sciences and Engineering Research Council of Canada Research, Equipment and Major Installation Grants to PČ, and Equipment and Infrastructure Grants to F. C. Hawthorne. The authors are indebted to M. A. Cooper for single-crystal X-ray diffraction study, J. B. Selway for a critical review of the manuscript, and to F. Fontan, C. Francis, A.-M. Fransolet and P. Keller for discussion of the poorly defined minerals; however, the responsibility for any misidentification rests solely with the authors.

Submitted January 27, 2000

References

Antenucci, D. – Fontan, F. – Fransolet, A.-M. (1989): X-ray powder diffraction data for wolfeite: (Fe$_{0.59}$ Mn$_{0.40}$ Mg$_{0.01}$)PO$_4$(OH). – Powder Diffraction 4, 34–35.

Appleman, D. E. – Evans, H. T., Jr. (1973): Job 9214: indexing and least-squares refinement of powder diffraction data. – U. S. Geol. Survey, Comput. Contrib. 20, NTIS Document PB-216188.

Čech, F. (1981): Pegmatites of Bohemia. *In:* J. H. Bernard et al., Mineralogy of Czechoslovakia, Academia Praha (in Czech).

Čech, F. – Paděra, K. – Povondra, P. (1961): Lipscombite from pegmatites at Otov near Domažlice (Bohemia, Czechoslovakia). – Acta Univ. Carolinae, Geol., No. 3, 145–157 (in Czech).

Fransolet, A.-M. – Antenucci, D. – Speetjens, J.-M. – Tarte, P. (1984): An X-ray determinative method for the divalent cation ratio in the triphylite – lithiophilite series. – Mineral. Mag., 48, 373–381.

Fransolet, A.-M. – Fontan, F. – Keller, P. (1995): Wyllieite and the aluminium-bearing alluaudites. – Berichte d. deutsch. Mineral. Gesellschaft No. 1, 1995, Beihefte z. Eur. Jour. Mineral., 7, 69 pp.

Fransolet, A.-M. – v. Knorring, O. – Fontan, F. (1992): A new occurrence of samuelsonite in the Buranga pegmatite, Rwanda. – Bull. Geol. Soc. Finland, 64, 13–21.

Frondel, C. (1949): Wolfeite, xanthoxenite and whitlockite from the Palermo mine, New Hampshire. – Amer. Mineral., 34, 692–705.

Moore, P. B. (1982): Pegmatite minerals of P(V) and B(III). *In:* P. Černý, ed., Granitic Pegmatites in Science and Industry, Mineral. Assoc. Canada Sh. Course Hbk. 8, 267–291.

Moore, P. B. – Araki, T. - Merlino, S. – Mellini, M. – Zanazzi, P. F. (1981): The arrojadite - dickinsonite series, K Na$_4$ Ca (Fe,Mn)$^{2+}_{14}$ Al (OH)$_2$ (PO$_4$)$_{12}$: crystal structure and crystal chemistry. – Amer. Mineral., 66, 1034–1049.

Moore, P. B. – Irving, A. J. – Kampf, A. R. (1975): Foggite, CaAl (OH)$_2$ (H$_2$O)[PO$_4$]; goedkenite, (Sr,Ca)$_2$ Al (OH) [PO$_4$]$_2$; and samuelsonite, (Ca,Ba) Fe$^{2+}_2$ Mn$^{2+}_2$ Ca$_8$ Al$_2$ (OH)$_2$ [PO$_4$]$_{10}$: three new species from the Palermo No. 1 pegmatite, North Groton, New Hampshire. – Amer. Mineral., 60, 957–964.

Moore, P. B. – Ito, J. (1979): Alluaudites, wyllieites, arrojadites: crystal chemistry and nomenclature. – Mineral. Mag., 43, 227–235.

Novák, M. – Černý, P. – Čech, F. – Staněk, J. (1992): Granitic pegmatites in the territory of the Bohemian and Moravian Moldanubicum. – Internat. Symp. Lepidolite 200, Nové Město na Moravě, Czechoslovakia, Field Trip Guidebook, 11–20.

Novotný, M. (1956): Phosphates from the pegmatite in Větrný vrch at Ohnišťovice. – Práce Brněn. základny ČSAV, 28, 10, 501–540 (in Czech).

Novotný, M. – Pokorný, J. – Staněk, J. – Štelcl, J. (1951): Triphylite from Větrná at Otov. – Čas. Nár. Musea, 120, 155–158 (in Czech).

Plimer, I. R. – Blucher, I. D. (1979): Wolfeite and barbosalite from Thackaringa, Australia. – Mineral. Mag., 43, 505–507.

Pouchou, J.-L. – Pichoir, F. (1984): A new model for quantitative analysis. I. Application to the analysis of homogeneous samples. – La Recherche Aerosp., 3, 13–38.

Pouchou, J.-L. – Pichoir, F. (1985): "PAP" (phi-rho-Z) procedure for improved quantitative microanalysis. In Microbeam Analysis (J. T. Armstrong ed.), San Francisco Press, San Francisco, California, 104–106.

Staněk, J. (1960): Montebrasite, augelite and lazulite from Otov. – Práce Brněn. základny ČSAV, 32, 1, 17–32 (in Czech).

Vejnar, Z. (1965): Pegmatites of the Poběžovice – Domažlice region. – Sborník geol. věd, lož. geol., 4, 7–84 (in Czech).

Weber, A. (1948): Phosphates from the pegmatites of s. w. Bohemia. – Rozpr. Čes. akademie, 58, 1, 1–9.

Metasomatický wolfeit a sdružené fosfáty z granitického pegmatitu Otov I v západních Čechách

Pegmatit Otov I, vystupující na Větrném vrchu u vesnice Otov v západních Čechách, náleží k beryl-columbit-fosfátovému subtypu granitických pegmatitů třídy vzácných prvků se vzácným spodumenem. Doposud bylo v tomto pegmatitu zjištěno dvacet fosfátů, a tato studie poskytla dvanáct dalších. Wolfeit je zde ustanoven jako významný metasomatický minerál s průměrnou hodnotou Mn/(Mn+Fe)(at.) 0,46, s obsahem F většinou nižším než detekční limit elektronové mikrosondy; α 1.741, β 1.743, γ 1.746, γ–α 0.005, (+)2V střední (počítaný 37°), a 12.327(3), b 13.225(3), c 9.845(2)Å, β 108°23', V 1522.95(47) Å^3. Primáním předchůdcem wolfeitu byl (I) arrojadit-dickinsonit se zrny zirkonu (s uzavřeninami uraninitu) a sfaleritu (s kapkovitým chalkopyritem). Arrojadit-dickinsonit byl nejprve prostoupen (II) žilkami velmi jemnozrnné asociace muskovitu, fosfátů Fe, Mn, Al, Ca, Mg, Li (lazulitu-scorzalitu, eosforitu, samuelsonitu?, trifylinu a montebrasitu) a velmi podřadného kalcitu. V následující etapě byla většina arrojaditu-dickinsonitu zatlačena (III) jemnozrnným wolfeitem, s podřadným intersticiálním a na fluor chudým hydroxylapatitem. Částečné zatlačení trifylinu alluauditem, hagendorfitem a fází UK-D bylo souběžné s wolfeitovou metasomatozou, a probíhalo na jejím předpolí. Pozdní nízkoteplotní zatlačování a žilkování, pronikající všemi předchozími asociacemi, dalo vznik ludlamitu, goyazitu, hydroxylchlorapatitu, fairfielditu? a chloritu?. Celá fosfátová asociace se vyznačuje nepatrným obsahem F, přítomností Cl v pozdních fázích, a nízkým oxidačním stupněm. Významné obsahy Ca, Mg, Sr a Cl a nepatrné stopy Ba nasvědčují podstatné kontaminaci boční gabbroidní horninou v magmatické i hydrotermální etapě.